GPC-based optical micromanipulation in 3D real-time using a single spatial light modulator

Peter John Rodrigo, Ivan R. Perch-Nielsen, Carlo Amadeo Alonzo and Jesper Glückstad

Optics and Plasma Research Department, Risø National Laboratory, DK-4000 Roskilde, Denmark
jesper.gluckstad@risoe.dk

http://www.ppo.dk

Abstract: Using a novel dual-beam readout with the generalized phase contrast (GPC) method, a multiple-beam 3D real-time micromanipulation system requiring only one spatial light modulator (SLM) has been realized. A theoretical framework for the new GPC scheme with two parallel illumination beams is presented and corroborated with an experimental demonstration. Three-dimensional arrays of polystyrene microbeads were assembled in the newly described system. The use of air immersion objective lenses with GPC-based optical trapping allowed the simultaneous viewing of the assemblies in two orthogonal bright-field imaging perspectives.

OCIS codes: (170.4520) Optical confinement and manipulation; (140.7010) Trapping; (230.6120) Spatial light modulators

References

1. A. Ashkin, "Acceleration and trapping of particles by radiation pressure," Phys. Rev. Lett. **24**, 156-159 (1970).
2. D. G. Grier, "A revolution in optical manipulation," Nature **424**, 810-816 (2003).
3. K. Dholakia and P. Reece, "Optical micromanipulation takes hold," Nano Today **1**, 18-27 (2006).
4. P. J. Rodrigo, V. R. Daria, and J. Glückstad, "Real-time three-dimensional optical micromanipulation of multiple particles and living cells," Opt. Lett. **29**, 2270-2272 (2004).
5. P. J. Rodrigo, V. R. Daria, and J. Glückstad, "Four-dimensional optical manipulation of colloidal particles," Appl. Phys. Lett. **86**, 074103 (2005).
6. M. Reicherter, T. Haist, E. U. Wagemann, and H. J. Tiziani, "Optical particle trapping with computer-generated holograms written on a liquid-crystal display," Opt. Lett. **24,** 608-610 (1999).
7. G. Sinclair, P. Jordan, J. Courtial, M. Padgett, J. Cooper, and Z. J. Laczik, "Assembly of 3-dimensional structures using programmable holographic optical tweezers," Opt. Express **12,** 5475-5480 (2004).
8. J. Glückstad and P. C. Mogensen, "Optimal phase contrast in common-path interferometry," Appl. Opt. **40**, 268-282 (2001).
9. J. W. Goodman, Introduction to Fourier Optics, Second Edition (McGraw-Hill, New York, 1996).
10. I. R. Perch-Nielsen, P. J. Rodrigo, and J. Glückstad, "Real-time interactive 3D manipulation of particles viewed in two orthogonal observation planes," Opt. Express **18,** 2852-2857 (2005).

1. Introduction

For objects with dimensions of a few nanometers up to micrometers, minute forces due to light-matter interaction are normally strong enough to influence the motion of the particles. It was first experimentally demonstrated by Ashkin that optical forces could be used to accelerate and even trap tiny objects [1]. Since then a great deal of progress has been achieved in optical trapping, both in its applications and technique development [2, 3]. For example, optical trapping and manipulation of ensembles of microparticles, which opens for promising themes of studies within colloid science and microbiology, are now viable using reconfigurable patterns of optical fields [4-7]. Reconfigurability of the confining optical potential landscapes is made feasible and of great ease with the use of computer-programmable spatial light modulators (SLM).

#76034 - $15.00 USD Received 12 October 2006; revised 5 December 2006; accepted 8 December 2006

The generalized phase contrast (GPC) method offers an energy-efficient means of producing arbitrary intensity patterns [8]. Recently, GPC has been employed in realizing a multiple-beam three-dimensional (3D) trapping system for interactive manipulation of a plurality of microscopic particles and cellular organisms in real-time [4, 5]. In these previous GPC-trapping architectures, multiple counterpropagating-beam (CB) traps were created using two addressable devices: a spatial light modulator (SLM), which provided the GPC system a reconfigurable input phase pattern (for *xy* position control of traps), and a spatial polarization modulator (SPM), which controlled the power ratio in each CB trap and thereby adjusted the axial position of each particle.

In this paper we demonstrate a GPC-trapping system that utilizes just one SLM to generate CB traps with adjustable power ratios. We employ a single GPC imaging setup for transforming phase into intensity patterns while the SLM provides two off-axis phase-encoding regions illuminated by two equally sized circular beams. Reconfigurable intensity patterns corresponding to the two independently addressable circular regions are relayed to the sample volume and form a dynamic array of CB traps.

The succeeding section outlines theoretical and experimental considerations exploring GPC with a dual-beam illumination. In section 3, we describe the schematic diagram of the proposed single-SLM, GPC-based micromanipulation system and show multiple-particle 3D trapping experiments achieved with it. Finally, we give our summary and some potential extensions of this work.

2. GPC system with two parallel input beams

In order to appreciate the optical engineering aspects of the single-SLM GPC-trapping system that we propose in this work, we first elaborate on the system's core component, which is the implementation of the GPC scheme with two parallel input beams. Consider a GPC 4*f* imaging setup with an object, $e(x,y)$, and a phase contrast filter (PCF), $H(f_x, f_y)$, amplitude transmission functions defined by

$$e(x,y) = \mathrm{circ}\left(\sqrt{(x+x_0)^2+y^2}\,/\Delta r\right)\exp\left(j\phi_1(x+x_0,y)\right) + \mathrm{circ}\left(\sqrt{(x-x_0)^2+y^2}\,/\Delta r\right)\exp\left(j\phi_2(x-x_0,y)\right), \quad (1)$$

$$H(f_x,f_y) = A\left[1+\left(BA^{-1}\exp(j\theta)-1\right)\mathrm{circ}\left(\sqrt{f_x^2+f_y^2}\,/\Delta f_r\right)\right], \quad (2)$$

where the two circ-functions in Eq. (1) represent two laterally shifted tophat beams (of identical radii Δr) reading out input phase patterns ϕ_1 and ϕ_2 written on regions R_1 and R_2 of the SLM, respectively, as shown in Fig. 1. The filter parameters *A* and *B* are the amplitude transmission coefficients outside and inside, respectively, of an on-axis circular region of radius Δf_r in the frequency space. A constant phase shift of θ is introduced to the on-axis focused light within the Δf_r radius.

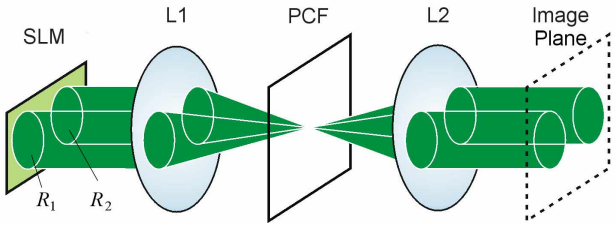

Fig. 1. 4*f* setup for implementing the GPC method with dual-beam illumination onto circular regions R_1 and R_2 of the spatial light modulator (SLM; Hamamatsu www.hamamatsu.com); PCF, phase contrast filter; L1 and L2, lenses (focal length = 300 mm).

#76034 - $15.00 USD Received 12 October 2006; revised 5 December 2006; accepted 8 December 2006

Assuming that a non-absorbing phase filter is used such that $A = B = 1$ and $\theta = \pi$, the field at the image plane of the 4*f* setup (neglecting space-inversion of the $x'y'$-coordinate system) is given by

$$\begin{aligned}\Im\{H(f_x, f_y)\Im\{e(x,y)\}\} &= \mathrm{circ}\left(\sqrt{(x'+x_0)^2 + y'^2}\,/\Delta r\right)\exp\left(j\phi_1(x'+x_0, y')\right) \\ &\quad - 2\overline{\alpha}_1\Im\left\{\mathrm{circ}\left(\sqrt{f_x^2 + f_y^2}\,/\Delta f_r\right)\Im\left\{\mathrm{circ}\left(\sqrt{x^2 + y^2}\,/\Delta r\right)\right\}\exp\left(j2\pi f_x x_0\right)\right\} \\ &\quad + \mathrm{circ}\left(\sqrt{(x'-x_0)^2 + y'^2}\,/\Delta r\right)\exp\left(j\phi_2(x'-x_0, y')\right) \\ &\quad - 2\overline{\alpha}_2\Im\left\{\mathrm{circ}\left(\sqrt{f_x^2 + f_y^2}\,/\Delta f_r\right)\Im\left\{\mathrm{circ}\left(\sqrt{x^2 + y^2}\,/\Delta r\right)\right\}\exp\left(-j2\pi f_x x_0\right)\right\} \quad (3)\end{aligned}$$

where

$$\overline{\alpha}_i = \left[\pi(\Delta r)^2\right]^{-1}\int_{R_i}\exp(j\phi_i)\mathrm{d}x\mathrm{d}y \quad ; \text{for } i = 1, 2. \quad (4)$$

From a previous theoretical analysis of the GPC method with single-beam illumination [8], it was found that the Fourier transform $\Im\left\{\mathrm{circ}\left(\sqrt{f_x^2 + f_y^2}\,/\Delta f_r\right)\Im\left\{\mathrm{circ}\left(\sqrt{x^2 + y^2}\,/\Delta r\right)\right\}\right\}$ represents a so-called synthetic reference wave (SRW), which is given by a circularly symmetric function $g(r')$:

$$\begin{aligned}g(r') &= \Im\{\mathrm{circ}(f_r/\Delta f_r)\Im\{\mathrm{circ}(r/\Delta r)\}\} \\ &= 2\pi\Delta r\int_0^{\Delta f_r} J_1(2\pi\Delta r f_r)J_0(2\pi r' f_r)\mathrm{d}f_r\,, \quad (5)\end{aligned}$$

where $r' = \sqrt{x'^2 + y'^2}$ and $f_r = \sqrt{f_x^2 + f_y^2}$. The similar Fourier transforms found in the second and the fourth terms on the right-hand side of Eq. (3), by the Shift Theorem [9], simply result in laterally displaced versions of the SRW. Thus from Eq. (3), the output intensity $I(x', y')$ at the image plane of the 4*f* setup is described by

$$I(x', y') = \left|e_1(x', y') + e_2(x', y')\right|^2, \quad (6)$$

where

$$e_1(x', y') = \mathrm{circ}\left(\sqrt{(x'+x_0)^2 + y'^2}\,/\Delta r\right)\exp\left(j\phi_1(x'+x_0, y')\right) - 2\overline{\alpha}_1 g\left(\sqrt{(x'+x_0)^2 + y'^2}\right) \quad (7)$$

and

$$e_2(x', y') = \mathrm{circ}\left(\sqrt{(x'-x_0)^2 + y'^2}\,/\Delta r\right)\exp\left(j\phi_2(x'-x_0, y')\right) - 2\overline{\alpha}_2 g\left(\sqrt{(x'-x_0)^2 + y'^2}\right). \quad (8)$$

The terms in the squared modulus of Eq. (6), strictly, combine coherently but if the chosen shift value x_0 is sufficiently large, the contributions of cross-product terms in the resultant intensity pattern become less significant. Therefore, the operation in Fig. 1 can be interpreted as two parallel GPC-based phase-to-intensity mappings that utilize the same PCF for their respective Fourier filtering processes.

Our above model of the two-beam input GPC exhibits good agreement with experimental results as shown in Fig. 2. We captured output intensity patterns by placing a CCD camera at the image plane depicted in Fig. 1. In the case of Fig. 2(a), the PCF is removed and we consequently obtain the profile of the two circular illumination beams (modeled as tophat beams). In the presence of an aligned PCF, made from glass optical flat with a tiny cylindrical pit (pit's depth corresponds to ~π phase shift and radius is ~7.5 μm [8]), phase-to-

#76034 - $15.00 USD Received 12 October 2006; revised 5 December 2006; accepted 8 December 2006

intensity conversion is achieved with good contrast as shown in Figs. 2(b) and 2(c). The encoded phase patterns on the SLM are arrays of dots with relative phase depths that may be selected on the fly between zero and π – corresponding to minimum and maximum intensity levels at the image plane. As quantified by the intensity line-scans of Fig. 2, we emphasize the approximately four-fold maximum intensity gain (ratio of intensity mapping of a π phase dot to incident intensity) due to the GPC method. In Fig. 2(b), a binary pattern consisting of π phase dots is used, resulting in duplicated intensity beam arrays, which may be used to form counterpropagating-beam traps with commensurate power ratios. CB traps with different power ratios can be synthesized from intensity patterns in Fig. 2(c) that uses multiple phase-levels on the SLM.

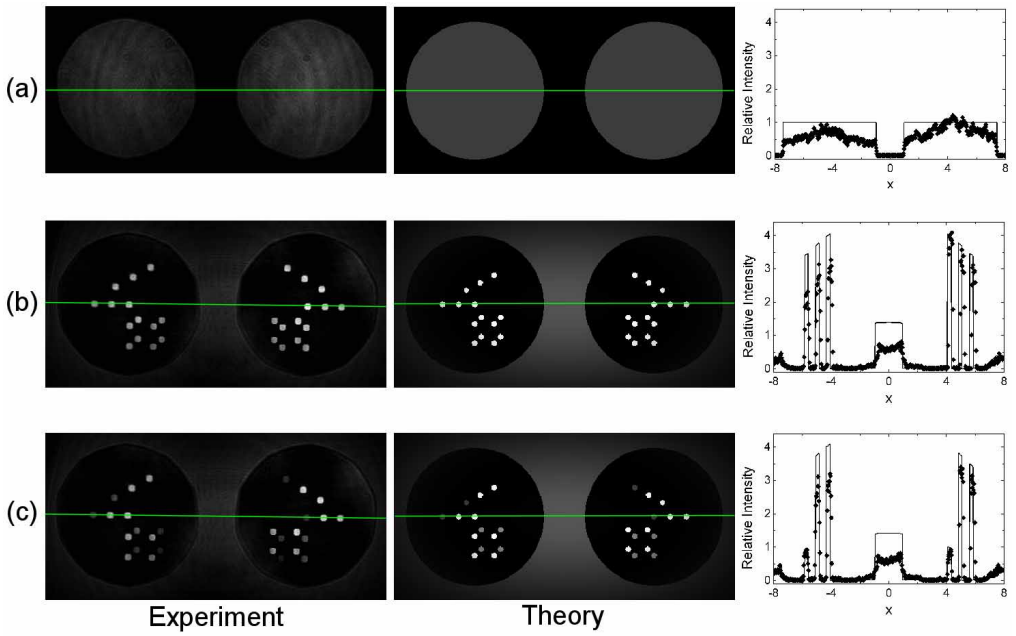

Fig. 2. Comparison of theoretically (solid curve in the line-scan) and experimentally obtained intensity patterns at the image plane of a GPC 4*f* setup with two adjacent input beams (modeled with tophat intensity profiles) (a) in the absence of the PCF, (b) with an aligned PCF and a binary phase-dot array input, and (c) with an aligned PCF and a multilevel phase-dot array input. Line-scans are taken along the green lines.

3. Single-SLM GPC-based optical trapping system

As an alternative to the use of a spatial polarization modulator to create modifiable counterpropagating-beam traps [4, 5], the optical trapping system reported here employs a GPC module with dual-beam readout shown in a folded geometry in Fig. 3. The two readout beams are made from twin images of a circular iris illuminated by an expanded beam from an Nd:YVO_4 laser (Laser Quantum Excel; wavelength = 532 nm; maximum power = 1.5 W) using a non-polarizing beam splitter and a right-angle mirror. The two sets of trapping intensity patterns produced at the image plane of the GPC setup are divided by a right-angle mirror and relayed to the sample region through identical long-working-distance low-NA objective lenses (Olympus LMPLFL) to form the array of CB traps. A graphical user-interface (GUI) using LabVIEW is designed to produce mirrored canvasses of phase patterns on the SLM and hence two coincident trapping intensity patterns at the sample region. The GUI also provides a user-friendly point-and-click and drag-and-drop features to interactively select and position CB traps along the *xy*-plane with overlaid real-time video data captured

#76034 - $15.00 USD Received 12 October 2006; revised 5 December 2006; accepted 8 December 2006

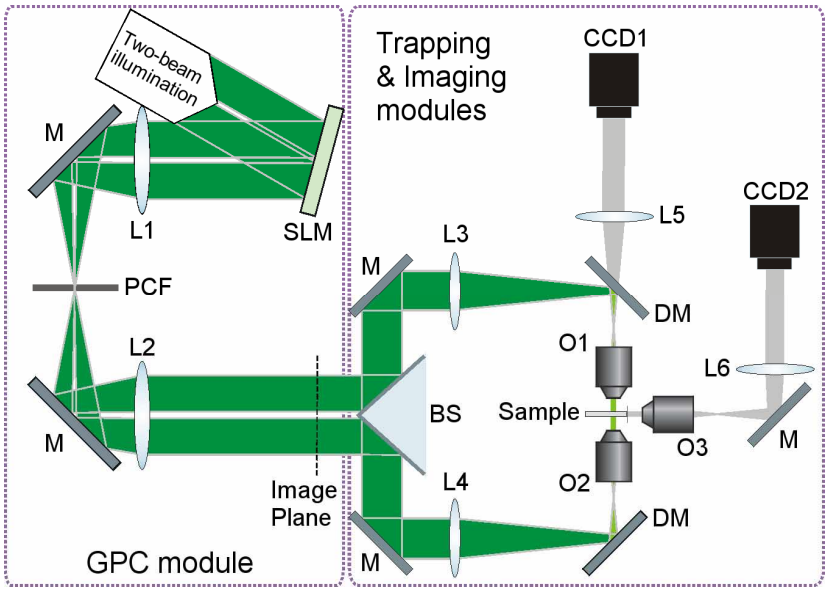

Fig. 3. Schematic diagram of the proposed optical micromanipulation system. SLM, spatial light modulator; PCF, phase contrast filter; M, mirror; L1 and L2, achromats (focal length = 300 mm); L3 and L4, achromats (focal length = 400 mm); L5 and L6, singlets (focal length = 300 mm and 200 mm, respectively); BS, beam splitter, DM, dicrhoic mirror; O1 and O2, trapping objective lenses (x50, NA = 0.55); O3, *yz*-view objective lens (x50, NA = 0.55); CCD1, *xy*-view camera; CCD2, *yz*-view camera.

through one of the trapping objective lenses. Adjustment in the power ratios of the CB traps are also implemented in the GUI using the multilevel phase encoding scheme described in the previous section.

One unique feature brought about by the use of low-NA (air immersion) objective lenses in the GPC-based trapping system is the capability to monitor the trapping volume in two perpendicular views [10]. In the previous demonstration of this imaging modality, we were able to achieve lateral (*xy*-plane) bright-field imaging and side (*yz*-plane) laser scatter imaging of the trapped particles. Here we extend the side-view imaging into bright-field mode. In Fig. 4, we show the simultaneously monitored *xy* and *yz* views of 3D-assemblies of microparticles held by CB traps.

Polystyrene microspheres have higher refractive index than the surrounding medium (i.e. water), and are attracted to regions of maximum lateral trap intensity. Thus, *xy*-plane manipulation of the particles is easily performed by repositioning the phase dots (and hence the CB traps) using the GUI. Meanwhile, the power ratio of the constituent beams of each CB trap is adjusted until the captured particle moves to a desired stable axial position.

In Fig. 4(a), three microspheres are stably trapped in distinct positions with a distance of ~30 μm axially separating the lowermost position from the topmost one. The *xy* coordinates of two particles are changed making the three beads appear diagonally arranged on both views as shown in Fig. 4(b). Finally, with eight CB traps, an array of microspheres is interactively assembled into a rhomboid structure.

Trapping of more than one particle along the axial direction can be done with GPC-system, as the user can axially stack up particles in a counterpropagating-beam trap if required. The so-called optical binding effect (particle interaction due to light-scattering) shows a possible means of controlling interparticle spacings axially. Alternatively, two or three beads may be axially positioned by holographic optical tweezers, but with limited interparticle spacings due to constraints of particle shadowing and spherical aberrations in a high-NA focusing objective with short confocal range [6, 7].

#76034 - $15.00 USD Received 12 October 2006; revised 5 December 2006; accepted 8 December 2006

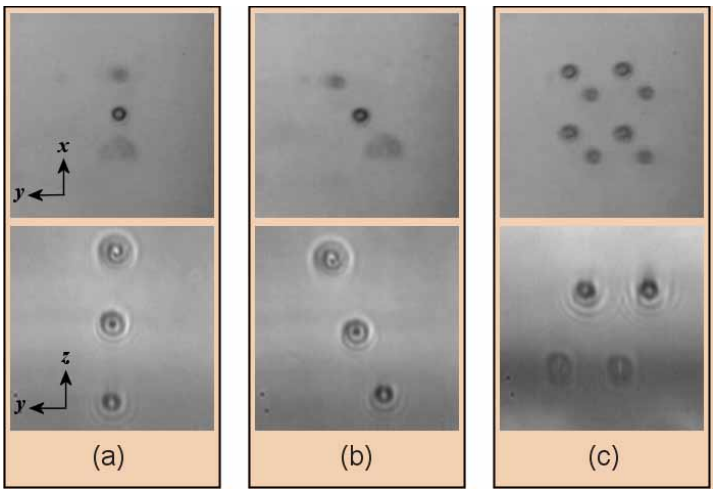

Fig. 4. Optically assembled arrays of 3-μm diameter polystyrene spheres in 3D simultaneously viewed in *xy* (top frame) and *yz* planes (bottom frame). (a)-(b) Two of three spheres are translated in the *xy*-plane. (c) Eight spheres optically positioned and stably kept in the corners of a virtual parallelepiped.

4. Conclusion

We have verified both theoretically and experimentally the viability of the GPC method with two parallel read-lights for 3D real-time micromanipulation. This implementation of the GPC setup enables the creation of a plurality of independently controllable counterpropagating-beam micromanipulators with the use of only a single SLM. We have also demonstrated two orthogonal bright-field image captures in the trapping system to allow more direct particle-position measurements through a genuine visual inspection of optically assembled microparticles in 3D.

The straightforward implementation of a bright-field mode in the side-view imaging module emphasizes the flexibility of the GPC-trapping system. Similar future extensions to the system could include other useful spectroscopic and imaging modalities (e.g. fluorescence, Raman). Notably, SLMs with rectangular displays like those based on liquid crystal on silicon (LCoS) technology provide more suitable aspect ratios for the synthesis of the twin trapping intensity patterns utilized in this system. Although the greater diffraction losses associated with commercially available LCoS-based SLMs need to be compensated with stronger laser sources, the advantage of higher resolutions, currently 1920×1080 pixels, can be gained from these devices. In fact, a single-SLM GPC-trapping system based on such a device would represent a resolution increase compared to previous double-SLM GPC-trapping systems using SLMs addressable to 480×480 pixels.

Due to its use of counterpropagating-beam trapping geometry, the GPC-based micromanipulation system's field of manipulation can be scaled to user-defined extents using a wide selection of objectives with different NA's. Note that for other trapping systems relying on tightly focused beam gradient-traps (e.g. holographic trapping [2, 3, 6, 7]), the manipulation range is limited due to the necessary use of oil or water immersion high-NA objectives.

Acknowledgments

We would like to thank the support from the EU-FP6-NEST program (ATOM3D), the ESF-Eurocores-SONS program (SPANAS) and the Danish Technical Scientific Research Council (FTP).

#76034 - $15.00 USD Received 12 October 2006; revised 5 December 2006; accepted 8 December 2006